



## Research Paper

# Passive thermal management system for downhole electronics in harsh thermal environments



Bofeng Shang, Yupu Ma, Run Hu<sup>\*</sup>, Chao Yuan, Jinyan Hu, Xiaobing Luo<sup>\*</sup>

State Key Laboratory of Coal Combustion, School of Energy and Power Engineering, Huazhong University of Science and Technology, Wuhan 430074, China

## HIGHLIGHTS

- A passive thermal management system is proposed for downhole electronics.
- Electronics temperature can be maintained within 125 °C for six-hour operating time.
- The result shows potential application for the logging tool in oil and gas industry.

## ARTICLE INFO

### Article history:

Received 15 October 2016

Accepted 26 January 2017

Available online 8 March 2017

### Keywords:

Downhole electronics

Harsh thermal environment

Passive thermal management system

Thermal insulation

Thermal storage

## ABSTRACT

The performance and reliability of downhole electronics will degrade in high temperature environments. Various active cooling techniques have been proposed for thermal management of such systems. However, these techniques require additional power input, cooling liquids and other moving components which complicate the system. This study presents a passive Thermal Management System (TMS) for downhole electronics. The TMS includes a vacuum flask, Phase Change Material (PCM) and heat pipes. The thermal characteristics of the TMS is evaluated experimentally. The results show that the system maintains equipment temperatures below 125 °C for a six-hour operating period in a 200 °C downhole environment, which will effectively protect the downhole electronics.

© 2017 Elsevier Ltd. All rights reserved.

## 1. Introduction

Due to the increasing demand for hydrocarbon resources, deeper and hotter wells are being explored worldwide. The oil and gas industries use a logging tool to detect the downhole viscosity, pressure and temperature, with required operating times of 4–6 h [1–4]. However, standard electronic components and sensors cannot effectively function for such long periods due to the harsh downhole environments. In general, the temperature and pressure in a downhole environment exceed 200 °C and 135 MPa, such that standard electronics quickly exceed their design temperatures (125 °C) [5,6]. Ongoing operation in such environments can degrade the detection performance as well as cause severe accidents. While the use of electronic components that can effectively operate at high temperatures would solve the temperature problem. However, the current options require expensive Silicon-On-Insulator (SOI) designs and die-attach materials [7–9].

A Thermal Management System (TMS) for the downhole electronics is currently more cost-effective and reliable than develop-

ing specialized electronic components. However, the harsh downhole conditions and the complex well logging structures have impeded the implementation of current TMS designs. Fig. 1 shows a well logging schematic. The logging tool burrows into the High-Temperature and High-Pressure (HTHP) muds that are thousands of meters deep. Hence, unlike conventional electronics [10–12], a downhole system needs to be hermetically sealed and protected from high pressures. Furthermore, the electronic components inside the system must be shielded from the corrosive downhole fluids. Various active cooling techniques have been proposed for thermal management, including thermoelectric cooling [5], vapor compression refrigeration [13], sorption cooling [14], convection cooling cycles [15], refrigerant circulation cooling [16] and thermoacoustic refrigeration [17]. These cooling techniques dissipate excess heat from the electronics into the surrounding downhole fluids. However, they generally require extra power, cooling liquids and other moving components, which further complicate the system.

In addition to active solutions, passive cooling technics have also been developed. Parrott et al. [18] proposed a passive cooling system that combined a Dewar flask with a heat sink. However, the overall thermal resistance between the electronics and the heat

<sup>\*</sup> Corresponding authors.

E-mail addresses: [hurun@hust.edu.cn](mailto:hurun@hust.edu.cn) (R. Hu), [Luoxb@hust.edu.cn](mailto:Luoxb@hust.edu.cn) (X. Luo).

### Nomenclature

$q$	heat transfer rate [mW]	$T_0$	initial temperature [°C]
$T$	temperature [°C]	$T_e$	final temperature [°C]
$V_T$	temperature rise rate [°C/s]	$\rho$	density [kg/m <sup>3</sup> ]
$P$	heating power [W]	$L$	latent heat of the PCM [kJ/kg]
$m$	mass [kg]	$u$	velocities in the x direction [m/s]
$m_{PCM}$	mass of the PCM [kg]	$v$	velocities in the y direction [m/s]
$c_p$	specific heat capacity [J/(kg·°C)]	$H$	specific enthalpy [J/kg]
$Q_s$	sensible heat [J]	$S$	heat generation rate [W/m <sup>3</sup> ]
$Q_L$	latent heat [J]		

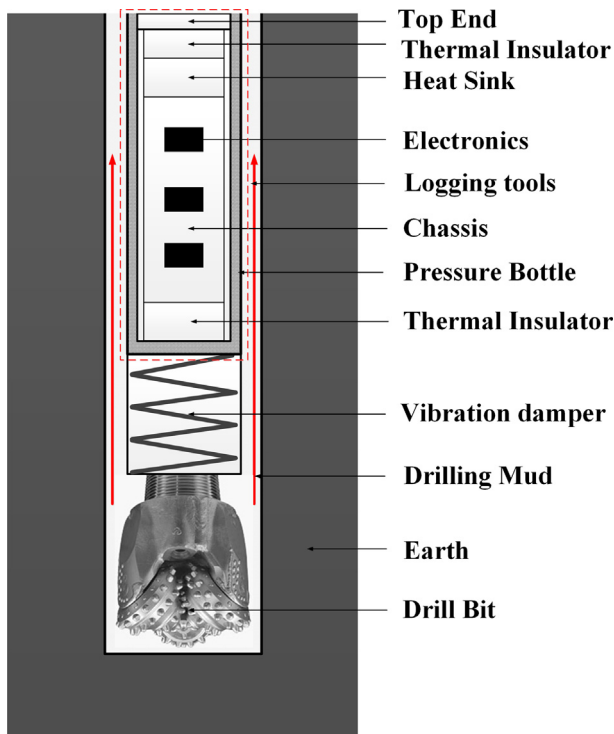


Fig. 1. Well logging schematic.

sink was quite large, resulting in a high temperature difference and a reduced reliability period for the electronic components. Jakaboski et al. [19] developed a closed coolant flow loop to provide a thermal path between the electronic components and the heat sink. However, the coolant pump and fluid expansion compensator complicated the system.

This paper describes a passive TMS inspired by existing down-hole electronics thermal management systems. A vacuum flask was employed to insulate the electronic components from the harsh external environment. The internal heat generation must also be transferred out of the components and stored elsewhere. Phase Change Materials (PCM) are viable thermal storage materials due to their significant latent heat capacity [20–24]. The TMS developed here used eutectic salts as the PCM. Heat pipes were used to provide an efficient heat transfer path from the electronic components to the PCM to reduce the temperature difference between them and, thereby, extend the viable operating time.

This study describes a passive TMS that uses a vacuum flask, a PCM and a heat pipe. The thermal characteristics of the present system is evaluated by experiments with a finite-element analysis for further validation.

## 2. Experimental setup

An experimental setup was designed to simulate practical operating conditions. Fig. 2(a) shows a schematic of the experimental setup. An oven created a high temperature environment with temperatures from 5 to 300 °C, with an accuracy of  $\pm 1$  °C. To insure uniform heating, two Teflon blocks were used to prevent direct contact between the logging tools and the oven. K-type thermocouples detected the electronic component temperatures to evaluate the TMS characteristics.

Fig. 2(b) shows a schematic of the original logging tool, which was comprised of a pressure bottle, electronic components, chassis, heat sink and adiabatic plug. Two resistance heaters (40 × 40 × 3 mm) were used as the electronic components. Thermal grease (FL-658) was used as the Thermal Interface Material (TIM) to attach the heaters onto the chassis. The grease thermal conductivity was approximately 3 W/(m·K). Fig. 2(c) shows a schematic of the logging tool with the TMS having a vacuum flask, heat pipes and the PCM.

The vacuum flask was made of titanium alloy, which could maintain a pressure of 1000 MPa. The flask was built of two concentric stainless steel tubes that were permanently cold-welded at both ends. The annular space between the tubes was evacuated at high temperature, providing an excellent barrier to heat transfer via conduction or convection. Both ends of the flask were sealed to reduce heat gain from the environment. The vacuum flask was 900 mm in length with inner and outer diameters of 73 and 90 mm.

The round heat pipe was made of copper with a length of 250 mm and a diameter of 5 mm. Water was used as the working fluid inside the pipe. The TMS had five heat pipes to connect the chassis to the PCM.

The PCM provided thermal storage for the electronic components and any heat gain into the vacuum flask. The low melting point and high latent heat of the PCM kept the electronic temperatures below their maximum temperature for a longer period. Therefore, the PCM selection is critical for the TMS characteristics. Eutectic salts, organic paraffin and eutectic metal alloys are common PCMs with high latent heats and low melting points. The PCM properties were evaluated to improve the system design.

Differential Scanning Calorimeter (DSC) tests were conducted to obtain the thermal properties and phase transition characteristics of the PCM, with a temperature rise rate of 5 °C/min. Fig. 3 shows the typical DSC curves. The PCM have different melting temperatures and different heat transfer rates with the latent heats calculated from the DSC test curves as:

$$L = \frac{\int_{Onset}^{End} q dT}{V_T m} \quad (1)$$

where  $q$  is the heat transfer rate,  $T$  is the temperature,  $V_T$  is the temperature rise rate, and  $m$  is the sample mass. *Onset* represents the

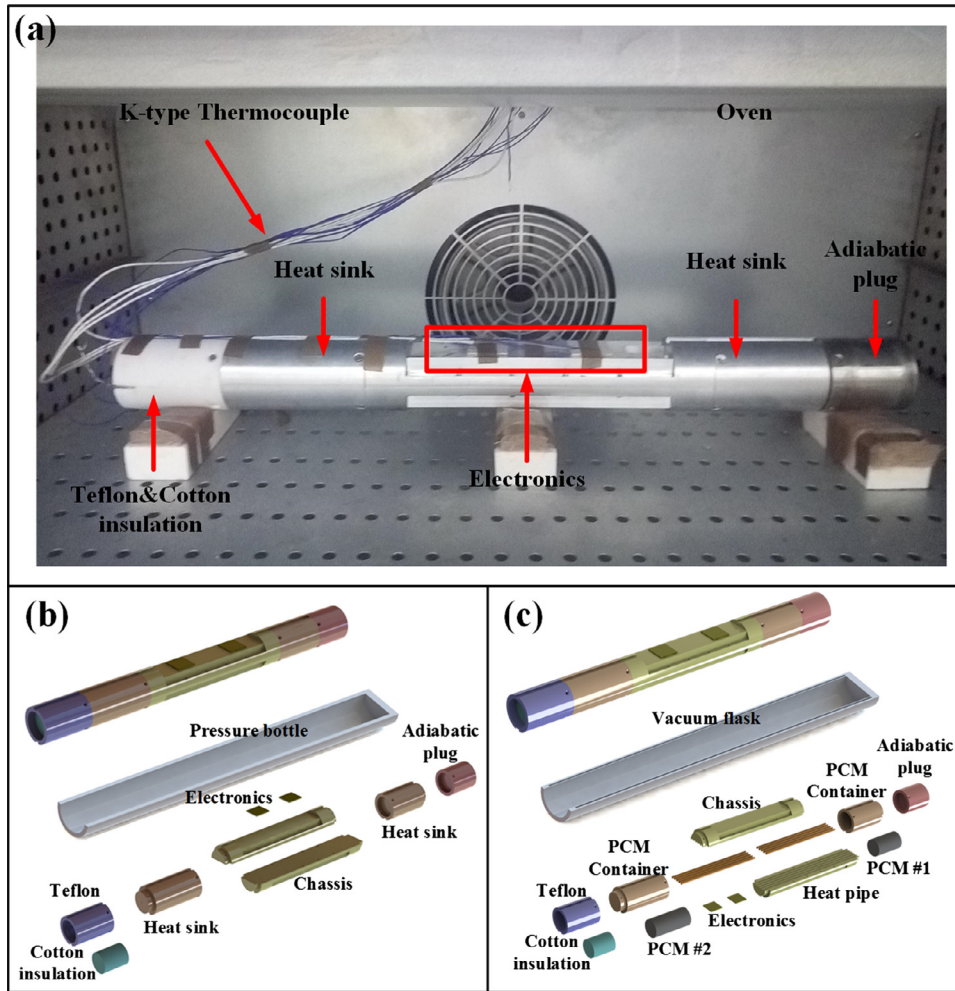


Fig. 2. Schematics for (a) experimental setup; (b) original logging tool; (c) logging tool with the TMS.

start of the temperature change and *End* represents the end of the temperature change. The top of the curve represents the melting point. A TC3000 (Xiotech) was used to measure the thermal conduc-

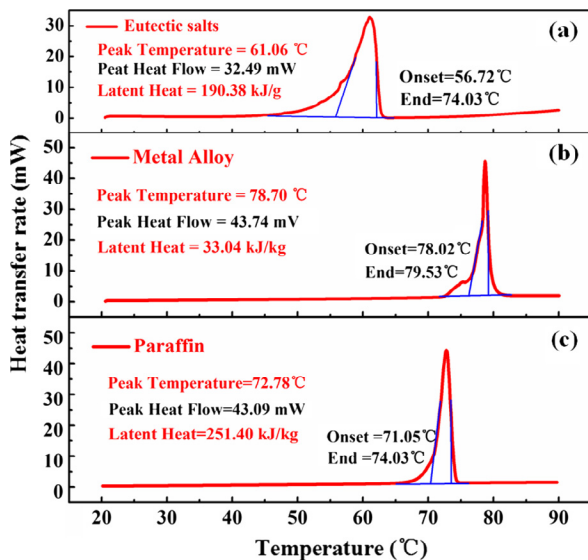


Fig. 3. DSC curve of different PCM (a) eutectic salts (b) eutectic metal alloy (c) organic paraffin.

tivities. Table 1 lists the properties of the different PCMs. The eutectic salts and the organic paraffin have higher latent heats than the eutectic metal alloy. However, the eutectic metal alloy has a much high thermal conductivity. A good PCM should have a high thermal conductivity and a high latent heat. However, where the overall system mass is limited, a larger mass impedes the logging system. Although the eutectic metal alloy has a significant thermal conductivity, a large mass is still required for the logging tool. Based on latent heat, thermal conductivity and mass considerations, the present study used the eutectic salts for the PCM.

The experiments were divided into three groups to highlight the effects of the vacuum flask, PCM and heat pipes on the electronic component temperatures. Two K-type thermocouples were attached to the surfaces of the electrical heaters and two more were inserted into the PCM. An additional thermocouple was fixed in the oven to measure the ambient temperature. The initial test temperature was room temperature. Table 2 lists the three experimental setups used to assess the thermal characteristics of the TMS.

### 3. Results and discussion

#### 3.1. Thermal insulation characteristics of the vacuum flask

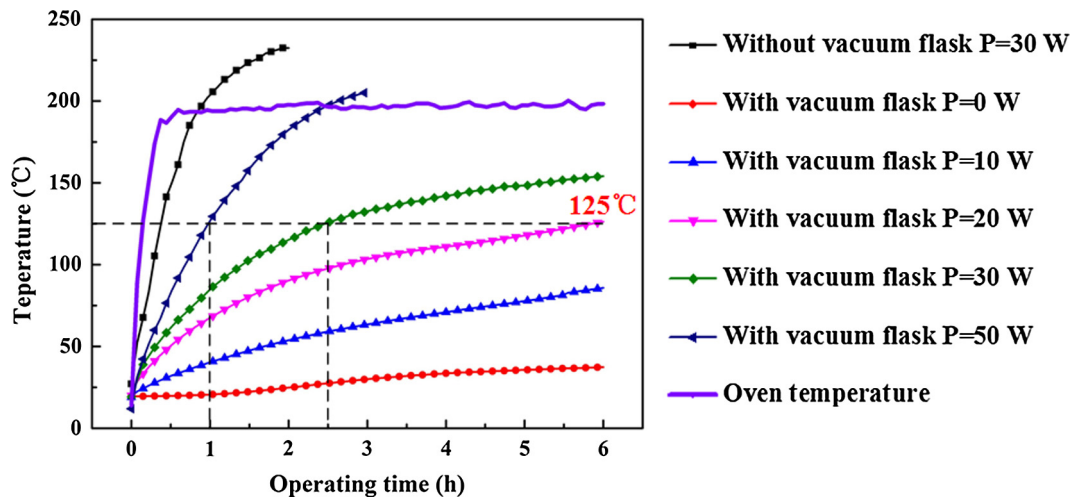
The Group 1 experiments assess the thermal insulation characteristics of the vacuum flask. Experiments were conducted with

**Table 1**  
PCM properties.

PCM	Melting point (°C)	Latent heat of fusion (kJ/kg)	Thermal conductivity (W/(m·K))	Density (kg/m <sup>3</sup> )	Specific heat, solid (J/(kg·K))	Specific heat, liquid (J/(kg·K))
Eutectic salts	61.1	190.4	0.50(s) 0.73(l)	1485	1930	1930
Metal alloy	78.7	33.04	18.8	9580	146	184
Organic paraffin	72.8	251.4	0.2	860	2000	2000

**Table 2**  
Experimental setups of different groups.

Group	Vacuum flask	PCM	Heat pipes	Boundary conditions
1	✓	×	×	P = 0–50 W
2	✓	✓	×	P = 30 W
3	✓	✓	✓	P = 30 W

**Fig. 4.** Electronic component temperatures for various heating powers.

and without the vacuum flask using heating powers ranging from 0 to 50 W to replicate the actual working conditions. Fig. 4 shows the electronic component temperatures at different heating powers. The temperatures exceed 125 °C after 0.38 h without the vacuum flask. The vacuum flask keeps the temperatures below 125 °C for 6 h for heating powers lower than 20 W. This indicates that the vacuum flask can prevent heat gain in a hot downhole environment. However, when the heating power exceeds 20 W, the operating time sharply decreases because the heat generated by the electronic components accumulates internally, which increases the component temperatures.

### 3.2. Thermal storage characteristics of the PCM

The Group 2 experiments analyze the thermal storage characteristics of the PCM. The PCM was 200 mm long and weighed 700 g. Fig. 5 compares the electronic component temperatures with and without the PCM. The results show that the electronic component temperatures are reduced from 154 °C to 124 °C by the PCM. The lower electronic component temperatures indicate that the PCM introduce additional thermal storage for the components so that the component temperatures rise less as the energy is

absorbed by the phase change process. The temperatures then remain stable at lower temperatures for an extended period, which improves component performance.

### 3.3. Thermal characteristics of the heat pipes

The Group 3 experiments investigated the effect of the heat pipes on the component temperatures. Fig. 6 compares the component temperatures with and without the heat pipes. The temperature is 125.7 °C without a heat pipe. The temperature difference between the components and the PCM is 17.5 °C which shows that the thermal storage capacity of the PCM is not fully utilized. After the heat pipes are added, the temperature difference between the components and PCM decreases to 5.5 °C, with a component temperature of 118.7 °C, a reduction of 7.0 °C. This confirms that the heat pipes provide an efficient heat transfer path from the components to the PCM.

### 3.4. System thermal characteristics

Fig. 7 shows the thermal characteristics of the TMS. The total power of the electronic components is 30 W. The PCM mass is

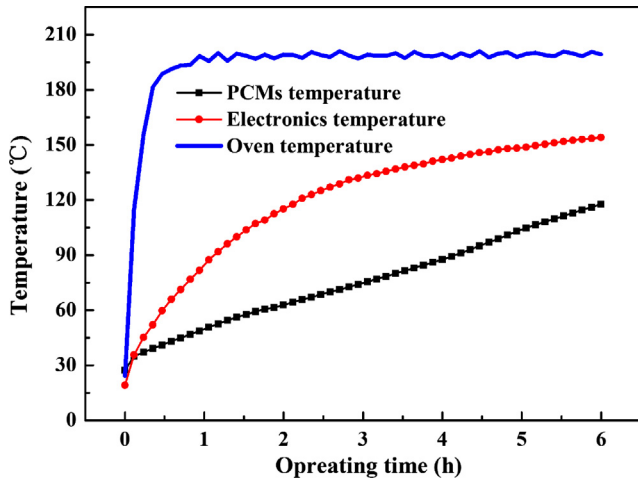


Fig. 5. Comparison of electronic component temperatures with and without PCM.

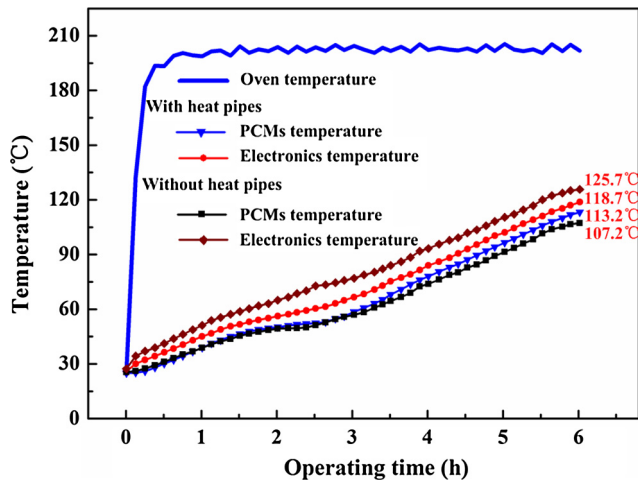


Fig. 6. Comparison of component temperatures with and without heat pipes.

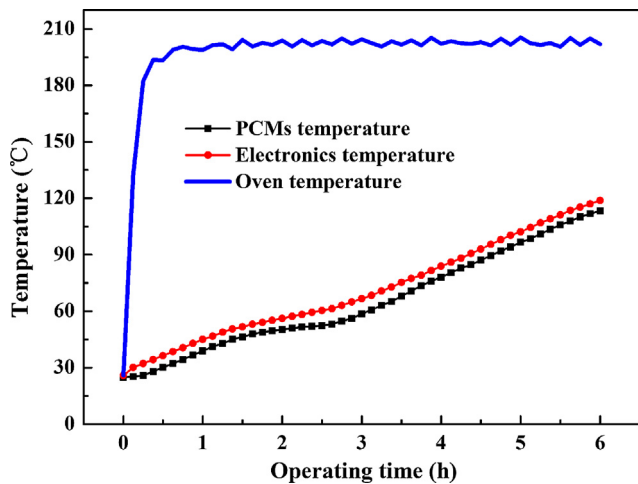


Fig. 7. TMS thermal characteristics.

700 g. The results show that the electronic component temperature is 119 °C after 6 h, indicating that the TMS effectively maintains the component temperature below 125 °C for an operating time of six hours. This result completely satisfies the requirements for the downhole electronic components.

### 3.5. Finite element analysis of the system thermal characteristics

The system thermal characteristics were then analyzed using a finite element analysis using COSOL Multiphysics as described in Appendix A using a two-dimensional symmetrical model. Fig. 8 (a) and (b) shows schematics of the physical model with and without the TMS. The boundary conditions were the same as those in the experiments. A heat transfer model was applied in the porous media to simulate the phase change process using a variable specific heat to represent the latent heat storage process to study the phase change thermal storage mechanism [25,26]. The model included the radiation term in the equivalent thermal conductivity, with the predictions compared with experimental data to confirm the accuracy.

Fig. 8(c) and (d) shows the temperature fields for both cases. The logging tool internal temperature with the TMS is lower than without the TMS where the electronic component temperatures exceed 200 °C within an hour. The results agree with the experimental data. Without the thermal insulation, the ambient heat immediately transfers into the logging tool through conduction and radiation due to the significant temperature difference between the tool and the environment.

The heat flow inside the logging tool was also investigated. Fig. 8(e) and (f) shows the simulated heat flux vectors near the electronics at 10 min where the arrow size is proportional to the heat flux. Without the TMS, heat is transferred from the heat sink to the electronic components, thus accelerating the temperature increase in the components. With the TMS, the heat dissipates from the electronic components to the PCM, which reduces the component temperatures. Although heat flows into the components from the pressure bottle side, there is almost no heat flow from the vacuum flask side, which further confirms the thermal insulation characteristics of the vacuum flask.

A qualitative analysis was conducted to further understand the lower temperatures of the electronic components with the TMS. Heat is gained from the environment and from the heat generated by the electronic components. The sensible heat increase is given by:

$$Q_s = mc_p(T_e - T_0) \tag{2}$$

The energy gained by the latent heat is given by:

$$Q_L = m_{PCM}L \tag{3}$$

where  $Q_s$  is the sensible heat storage,  $Q_L$  is the latent heat storage,  $m$  is the mass,  $C_p$  is the constant specific heat,  $T_0$  is the initial temperature,  $T_e$  is the final temperature and  $L$  is the latent heat of the PCM. The heat transfer is the difference between the thermal storage and the heat generated by the electronic components. Fig. 9 shows the heat output and the thermal storage for both cases. The TMS reduces the heat gain by 37.6%, which reduces the thermal storage. Per Eq. (1),  $T_e$  decreases as  $Q_s$  decreases. The PCM absorb 20.7% of the thermal storage, which results in a lower electronic component temperature.

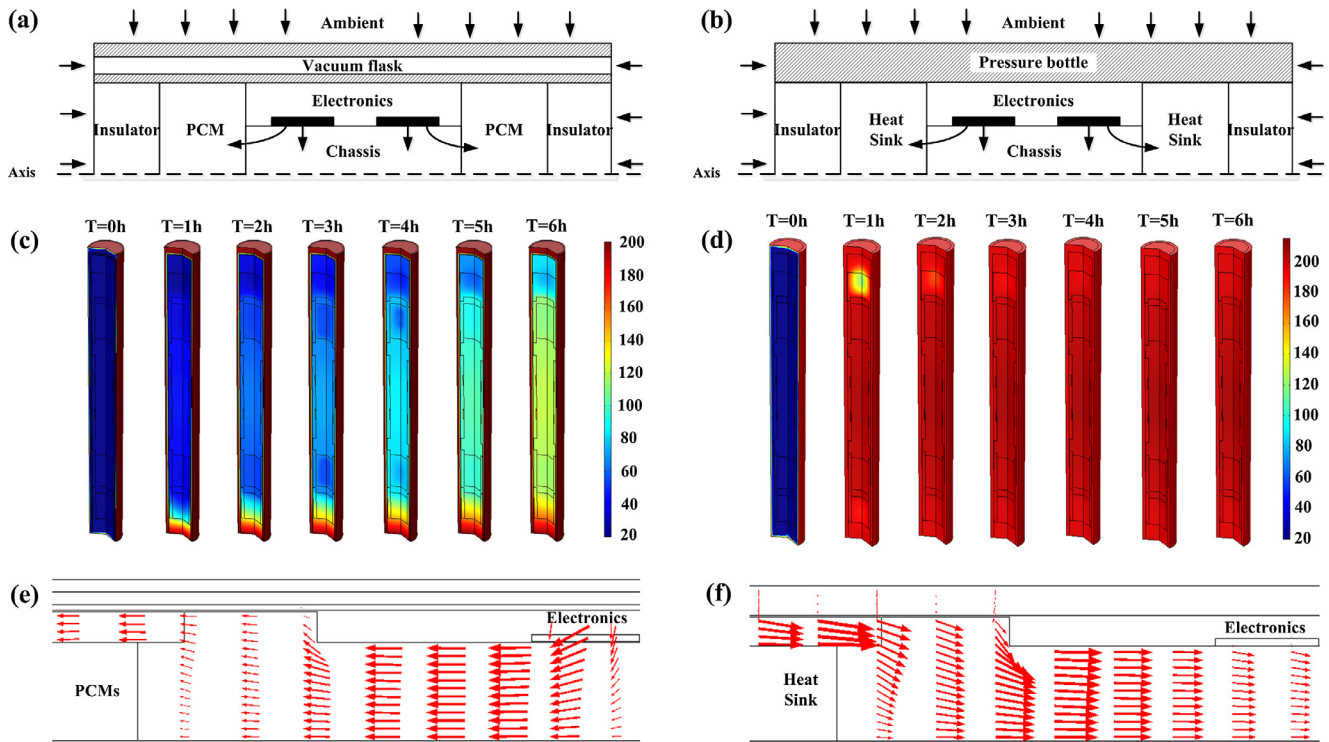


**Fig. 8.** Schematic diagram of the physical model (a) with TMS, (b) without TMS, (c) Case 1: temperatures with the TMS, (d) Case 2: temperatures without the TMS, (e) Case 1: simulated heat flux vectors near the electronic components at 10 min, (f) Case 2: simulated heat flux vectors near the electronic components at 10 min.

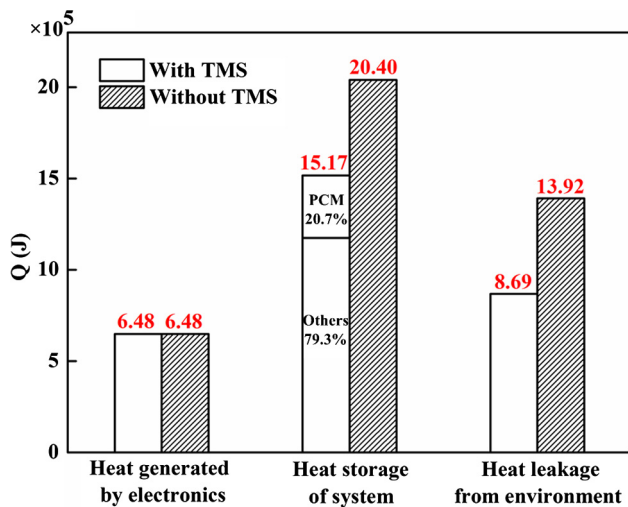


**Fig. 9.** Heat output and thermal storage of systems with and without TMS.

#### 4. Conclusions

This paper presents a passive TMS for downhole electronics in harsh thermal environments. The thermal insulation characteristics of a vacuum flask were experimentally evaluated. The results show that the flask efficiently reduces heat transfer from the hot downhole environment and the system cannot control the electronic component temperature for component power levels up to 20 W. When the flask is used with the PCM, the electronic component temperature is reduced by 30 °C. The heat pipes reduce the temperature difference between the electronic components and the PCM by 10.7 °C. Thus, the electronic component temperature

is maintained below 125 °C for a six-hour operating period. Thus, the presented TMS is a promising candidate for applications in the oil and gas industries.

#### Acknowledgment

The authors gratefully acknowledge financial support from the National Natural Science Foundation of China (Grant nos. 51625601, 51576078 and 51606074) and the Fundamental Research Funds for the Central Universities (2016JCTD112). Special thanks also goes to Ms. Wang Lin for assistance with the DSC test.

#### Appendix A

##### A.1. Governing equations

The following assumptions are made to simplify the calculations:

- (1) One-dimensional heat conduction based on Fourier's law;
- (2) The temperature outside the flask is the same as the down-hole temperature;
- (3) The heat generation in the PCB is symmetric and uniform;
- (4) No thermal convection inside the flask;
- (5) Gravity has no effect on the heat transfer.

The governing equations are:  
Continuity equation

$$\frac{\partial \rho}{\partial t} + \frac{\partial(\rho u)}{\partial x} + \frac{\partial(\rho v)}{\partial y} = 0 \quad (4)$$

where  $\rho$  is the PCM density, and  $u$  and  $v$  are the velocities in the  $x$  and  $y$  directions.

## Momentum equations

$$\rho \left[ \frac{\partial u}{\partial t} + u \frac{\partial u}{\partial x} + v \frac{\partial u}{\partial y} \right] = u \left[ \frac{\partial^2 u}{\partial x^2} + \frac{\partial^2 u}{\partial y^2} \right] - \frac{\partial p}{\partial x} + S_u \quad (5)$$

$$\rho \left[ \frac{\partial v}{\partial t} + u \frac{\partial v}{\partial x} + v \frac{\partial v}{\partial y} \right] = v \left[ \frac{\partial^2 v}{\partial x^2} + \frac{\partial^2 v}{\partial y^2} \right] - \frac{\partial p}{\partial y} + S_v \quad (6)$$

where  $S_u$  and  $S_v$  represent the appropriate momentum sink terms which account for the pressure drop caused by the porous solid material.

## Energy equation

$$\rho \left( \frac{\partial H}{\partial t} + u \frac{\partial H}{\partial x} + v \frac{\partial H}{\partial y} \right) = \frac{k}{c_p} \left( \frac{\partial^2 H}{\partial x^2} + \frac{\partial^2 H}{\partial y^2} \right) + S_h \quad (7)$$

where  $H$  represents the specific enthalpy and  $S_h$  is the heat generation rate:

$$S_h = \frac{\rho}{c_p} \frac{\partial(\Delta H)}{\partial t} \quad (8)$$

## References

- [1] J. Boyes, The eyes of the oil industry, *Electron. Power* 27 (1981) 484–488.
- [2] N.J. Hyne, *Nontechnical Guide to Petroleum Geology, Exploration, Drilling, and Production*, PennWell Books, 2012.
- [3] W.L. Cheng, Y.L. Nian, T.T. Li, C.L. Wang, A novel method for predicting spatial distribution of thermal properties and oil saturation of steam injection well from temperature logs, *Energy* 66 (2014) 898–906.
- [4] Q.M. Zhao, J.C. Fan, D. Yan, R.R. Tian, B. Zhou, C. Li, Development of downhole tools for stratified testing in oil and gas open-hole wells, *Adv. Mater. Res., Trans. Tech. Publ.* 422 (2012) 614–618.
- [5] M.R. Werner, W.R. Fahrner, Review on materials, microsensors, systems and devices for high-temperature and harsh-environment applications, *IEEE Trans. Ind. Electron.* 48 (2001) 249–257.
- [6] A. Sinha, Y.K. Joshi, Downhole electronics cooling using a thermoelectric device and heat exchanger arrangement, *J. Electron. Pack.* 133 (2011) 041005.
- [7] B. Tian, H. Liu, N. Yang, et al., Note: high temperature pressure sensor for petroleum well based on silicon over insulator, *Rev. Sci. Instrum.* 86 (2015) 126103.
- [8] B.W. Ohme, B.J. Johnson, M.R. Larson, *SOI CMOS for Extreme Temperature Application*, Honeywell Aerospace, Defense & Space, Honeywell International, 2012.
- [9] J.L. Evans, P. Lall, R. Knight, E. Crain, T. Shete, J.R. Thompson, System design issues for harsh environment electronics employing metal-backed laminate substrates, *IEEE Trans. Comp. Pack. Technol.* 31 (2008) 74–85.
- [10] C. Yuan, L. Li, B. Duan, B. Xie, Y.M. Zhu, X.B. Luo, Locally reinforced polymer-based composites for efficient heat dissipation of local heat source, *Int. J. Therm. Sci.* 102 (2016) 202–209.
- [11] C. Yuan, B. Xie, M.Y. Huang, R.K. Wu, X.B. Luo, Thermal conductivity enhancement of platelets aligned composites with volume fraction from 10% to 20%, *Int. J. Heat Mass Transfer* 94 (2016) 20–28.
- [12] X.B. Luo, R. Hu, S. Liu, K. Wang, Heat and fluid flow in high-power LED packaging and applications, *Prog. Energy Combust. Sci.* 56 (2016) 1–32.
- [13] A.G. Flores, Apparatus and Method for Actively Cooling Instrumentation in a High Temperature Environment, US Patent 5,701,751, Dec. 30, 1997.
- [14] R. DiFoggio, Downhole Sorption Cooling of Electronics in Wireline Logging and Monitoring while Drilling, US Patent 6,341,498, Jan. 29, 2002.
- [15] F.S. Martin, J.L. Bearden, Downhole Motor Cooling and Protection System, US Patent 5,554,897, Sep. 10, 1996.
- [16] K.S. De, Downhole Tool Cooling System, US Patent 4,407,136, Oct. 4, 1983.
- [17] G.A. Bennett, Active Cooling for Downhole Instrumentation: Miniature Thermoacoustic Refrigerator (Ph.D. Thesis), The University of New Mexico, New Mexico, 1991.
- [18] R.A. Parrott, H. Song, K. Chen, Cooling System for Downhole Tools, US Patent 6,336,408, Jan. 8, 2002.
- [19] J.C. Jakaboski, Innovative Thermal Management of Electronics Used in Oil-well Logging (MS Thesis), Georgia Institute of Technology, Atlanta, 2004.
- [20] R. Kandasamy, X. Wang, A.S. Mujumdar, Application of phase change materials in thermal management of electronics, *Appl. Therm. Eng.* 27 (2007) 2822–2832.
- [21] Z.C. Wang, Z.Q. Zhang, J. Li, L.X. Yang, Paraffin and paraffin/aluminum foam composite phase change material heat storage experimental study based on thermal management of Li-ion battery, *Appl. Therm. Eng.* 78 (2015) 428–436.
- [22] Y. Tomizawa, K. Sasaki, A. Kuroda, R. Takeda, Y. Kaito, Experimental and numerical study on phase change material (PCM) for thermal management of mobile devices, *Appl. Therm. Eng.* 98 (2016) 320–329.
- [23] J.T. Zhao, Z.H. Rao, C.Z. Liu, Y.M. Li, Experimental investigation on thermal performance of phase change material coupled with closed-loop oscillating heat pipe (PCM/CLOHP) used in thermal management, *Appl. Therm. Eng.* 93 (2016) 90–100.
- [24] J.Y. Hu, R. Hu, Y.M. Zhu, X.B. Luo, Experimental investigation on composite phase-change material (CPCM)-based substrate, *Heat Transfer Eng.* 37 (2016) 351–358.
- [25] V.S.S. Srinivas, G.K. Ananthasuresh, Analysis and topology optimization of heat sinks with a phase-change material on COMSOL Multiphysics™ platform, in: *COMSOL Users Conference*, 2006, pp. 1–7.
- [26] A.H. Mosaffa, L.G. Farshi, C.A.I. Ferreira, M.A. Rosen, Energy and exergy evaluation of a multiple-PCM thermal storage unit for free cooling applications, *Renew. Energy* 68 (2014) 452–458.